Heliyon 10 (2024) e24159

Contents lists available at ScienceDirect

Heliyon

journal homepage: www.cell.com/heliyon

Research article

Wall panel structure design optimization of a hexagonal satellite

Reham Reda [a,*], Yasmeen Ahmed [a], Islam Magdy [a], Hossam Nabil [a], Mennatullah Khamis [a], Mohamed Abo Lila [a], Ahmed Refaey [a], Nada Eldabaa [a], Manar Abo Elmagd [a], Adham E. Ragab [b], Ahmed Elsayed [c]

[a] Department of Mechanical Engineering, Faculty of Engineering, Suez University, P.O.Box: 43221, Suez, Egypt
[b] Department of Industrial Engineering, College of Engineering, King Saud University, P.O. Box 800, Riyadh, 11421, Saudi Arabia
[c] Advanced Forming Research Centre, Strathclyde University, Renfrew, Glasgow, PA4 9LJ, Scotland

ARTICLE INFO

Keywords:
Wall panel structure
Isogrid structure
Honeycomb structure
Mechanical performance
Vibration behavior
Simulation and validation
Manufacturing and assessment

ABSTRACT

Considering that it satisfies high strength and stiffness at a low weight, the grid structure is the ideal option for meeting the requirements for developing the wall panel structure for the satellite. The most attractive grid structures for the satellite wall panel industry are isogrid and honeycomb structures. The first part of this work involves studying the mechanical and dynamic performance of five designs for the satellite wall panel made of 7075-T0 Al-alloy. These designs include two isogrid structures with different rib widths, two honeycomb structures with different cell wall thicknesses, and a solid structure for comparison. The performance of these designs was evaluated through compression, bending, and vibration testing using both finite element analysis (FEA) with the Ansys workbench and experimental testing. The FEA results are consistent with the experimental ones. The results show that the isogrid structure with a lower rib thickness of 2 mm is the best candidate for manufacturing the satellite wall panel, as this design reveals the best mechanical and dynamic performance. The second part of this work involves studying the influence of the length of the sides of the best isogrid structure in the range of 12 mm–24 mm on its mechanical and dynamic performance to achieve the lowest possible mass while maintaining the structure's integrity. Then, a modified design of skinned wall panels was introduced and dynamically tested using FEA. Finally, a CAD model of a hexagonal satellite prototype using the best-attained design of the wall panel, i.e., the isogrid structure with a 2 mm rib width and 24 mm-long sides, was built and dynamically tested to ensure its safe design against vibration. Then, the satellite prototype was manufactured, assembled, and successfully assessed.

1. Introduction

The satellite is exposed to a wide range of loading circumstances during the several phases of a launch, including mechanical shocks, dynamic loading, and static loading. The loading conditions must be recognized and computed to prevent plastic deformations and failures. Static loading includes thermal loads, like the rocket's air resistance and the engine's temperature rise, in addition to stresses induced during component assembly and longitudinal and lateral accelerations in a stable condition through departure. Dynamic external loads during takeoff could include the power of the engine, loud pressure, air speeds, and vibrations during transport to the launch location. Mechanisms for separation that allow the release of the satellite cause mechanical shocks. As a result, the

* Corresponding author.
E-mail address: Reham.reda@suezuni.edu.eg (R. Reda).

https://doi.org/10.1016/j.heliyon.2024.e24159
Received 12 September 2023; Received in revised form 31 December 2023; Accepted 4 January 2024
Available online 7 January 2024

satellite's mechanical structure needs to be able to withstand the mechanical pressures that it must endure [1,2].

The choice of materials is one of the most important stages in the design of a satellite structure. When developing the satellite's mechanical structure, a number of material requirements need to be taken into account, including specific stiffness, specific strength, thermal conductivity and thermal expansion coefficients, manufacturability, cost, and out-gassing characteristics [3]. Aluminum alloys are the most widely used metallic materials in the fabrication of satellite wall panels because of their excellent workability, high ductility, resistance to corrosion, high stiffness-to-density ratios, high strength-to-weight ratios, lack of magnetism, ease of machining, and affordable price. 7075-T Al-alloy is the most popular space-grade material that satisfies the requirements according to the NASA list of satellite materials [1,2,4].

For the satellite structure, the grid structures are promising in terms of enhancing the strength-to-weight ratio and maintaining the stiffness of the wall panels at the lowest weight, which reduces manufacturing and launch costs. Moreover, reducing the total mass of the satellite exhibits many other merits, such as facilitating the assembly of the whole satellite and the deployment of large-scale structures in orbit, such as solar arrays and antennas, which can expand the capabilities and applications of space technology. In addition, it permits increasing the payload capacity of rockets and satellites, which can enable more ambitious missions [1–3].

This work deals with two configurations of the grid structures, i.e., isogrid and honeycomb structures. Both structures can be manufactured using CNC machining processes. Because of the incredibly high degree of precision demanded by the aerospace sector, CNC machining is regarded as an outstanding manufacturing technology. Using this method, incredibly tight tolerances can be acquired. Consequently, it uses robust metallic and plastic components to produce excellent resolution and aircraft functionality [1,2]. Both grid structures are employed as a thicker core that is adhesively bonded to an upper and/or lower thin skin solid layer to form the sandwich panel structure. The sandwich panel has isotropic strength characteristics, meaning it has equal properties measured in any direction [1,5]. Therefore, these grid structures need to be thick enough to give high shear stiffness to prevent panel buckling, as well as having enough normal flexural shear strength to sustain shear and flexural loads [1,6,7].

The isogrid structure configuration utilizes an array of equal-length triangle cutouts to promote the stiffness per weight of a wall panel, saving material and therefore weight, as the mass of the satellite application was reduced by 70% [1,2]. The geometric variables of the isogrid structure include rib width, thickness, and height [1,5,8]. In the instance where this structure experiences an axial compressive load, the failure could result from either local buckling in the case where the ribs are thinner than the panel or global buckling in the case where the panel is thinner than the ribs [1,5,9]. The isogrid structure can enhance the buckling resistance and mechanical performance of the structure by controlling the design of the ribs [2,5,10]. A limited number of research works have studied isogrid structure design optimization [2–6,8–13].

Zheng et al. [11] used FEA to optimize a stiffened cylinder with a 6 m height and 4 m diameter. They claimed that the rib thickness ought to exceed the rib width because of the quadratic relationship between critical force and thickness. Dawood et al. [12] studied the influence of the isogrid structure on the natural frequencies of the structure. They claimed that the natural frequencies measured for the isogrid structure situation were higher than those for the solid structure case because of the isogrid structure's smaller mass; however, this is only true if the stiffness remains constant. The influence of rib thickness and width on the strength of polyamide reinforced with 20% of the weight of short carbon fiber was examined by Ciccarelli et al. [8]. They observed that the increase in rib thickness enhances both overall and particular strength, and the increase in rib width decreases the specific strength and promotes the overall strength. Additionally, they observed that isogrid structures may rupture under local or global buckling, relying on the geometric variables, and that isogrid structures with a local buckling failure mode have a lower specific strength than expected. Forcellese et al. [13] produced isogrid panels in short carbon fiber-reinforced polyamide with different rib thickness and rib height values using additive manufacturing. They investigated the effects of these geometric variables on the compressive strength and buckling behavior of the isogrid panels through compression testing. Researchers observed that raising the rib height decreases the maximum load and a specific maximum load, while increasing the rib width generates an increase in peak load and a maximum load. Additionally, they noticed that the isogrid panel failed upon compression testing as a result of the global buckling failure mode, suggesting that the structure's slenderness is greater than that of a rib. Forcellese et al. [14] also conducted research on the buckling and environmental performance of composite structures made via 3D printing. They included dried isogrid structures with 3 mm and 5 mm rib widths, solid, and dried solid in their comparison. They observed that the isogrid structure with a 3 mm rib width showed the lowest buckling resistance and environmental pressures. In terms of buckling resistance, the solid and isogrid structures' outcomes with dry panels with a 5 mm rib width are rather similar. The environmental costs of the latter, however, are greater than those of the former.

The honeycomb structure is the other grid structure configuration, which is thought to be the lightest option in instances where there is compressive or bending loading [15]. The geometric variables of the honeycomb structure that affect the mechanical performance are cell wall thickness, size, and height [16]. The influence of these variables on compressive strength, crushing strength, and forced vibration has been studied in a limited number of studies [15–20]. Abd Kadir et al. [17] performed a numerical study of the crushing strength of Kraft paper honeycomb under compression loading with different cell wall thickness, cell size, and density. They noticed that when cell size reduces, crushing strength rises, and that the highest strength was attained with a 10 mm cell size and a 0.4 mm cell wall thickness. Sadiq et al. conducted an experimental and numerical investigation to determine the effect of honeycomb design variables on the forced vibration behavior of aircraft sandwiches with honeycomb cores [16]. Thomas and Tiwari developed some noteworthy observations on the quasi-static and dynamic crushing responses of honeycomb structures [19]. They observed that an increase in cell wall thickness (0.8–1.5 mm) results in a higher maximal transient response, whereas an increase in core height (5–25 mm) has the opposite effect. They also stated that the greatest transient response was negatively impacted by growing cell size. Their results show that cell wall thickness has a smaller effect and that core height fluctuation has a larger effect than the other variables. Geometrical variables like cell size, node length, cell wall thickness, and cell layout affected the honeycomb core's performance under static pressures applied in different directions. The honeycomb cell configurations in hexagon, triangle, square, and

circular shapes were selected with the least amount of material needed and the highest strength requirements in mind. A hexagonal honeycomb was the best design for both the greatest strength and the least amount of material [19].

The literature described above indicates that there is a lack of research examining how structural geometry variables affect the mechanical and vibration behavior of the key aerospace alloy 7075 Al-alloy. To find the best design for a satellite wall panel that meets the dynamic behavior requirements of satellites and achieves a high strength-to-weight ratio, the current work examines the effects of various grid structure designs, such as isogrid, honeycomb, and solid structures, on the compression, bending, and vibration behaviors. The best-attained-performance wall panel design was further improved. Furthermore, a prototype of a hexagonal satellite structure

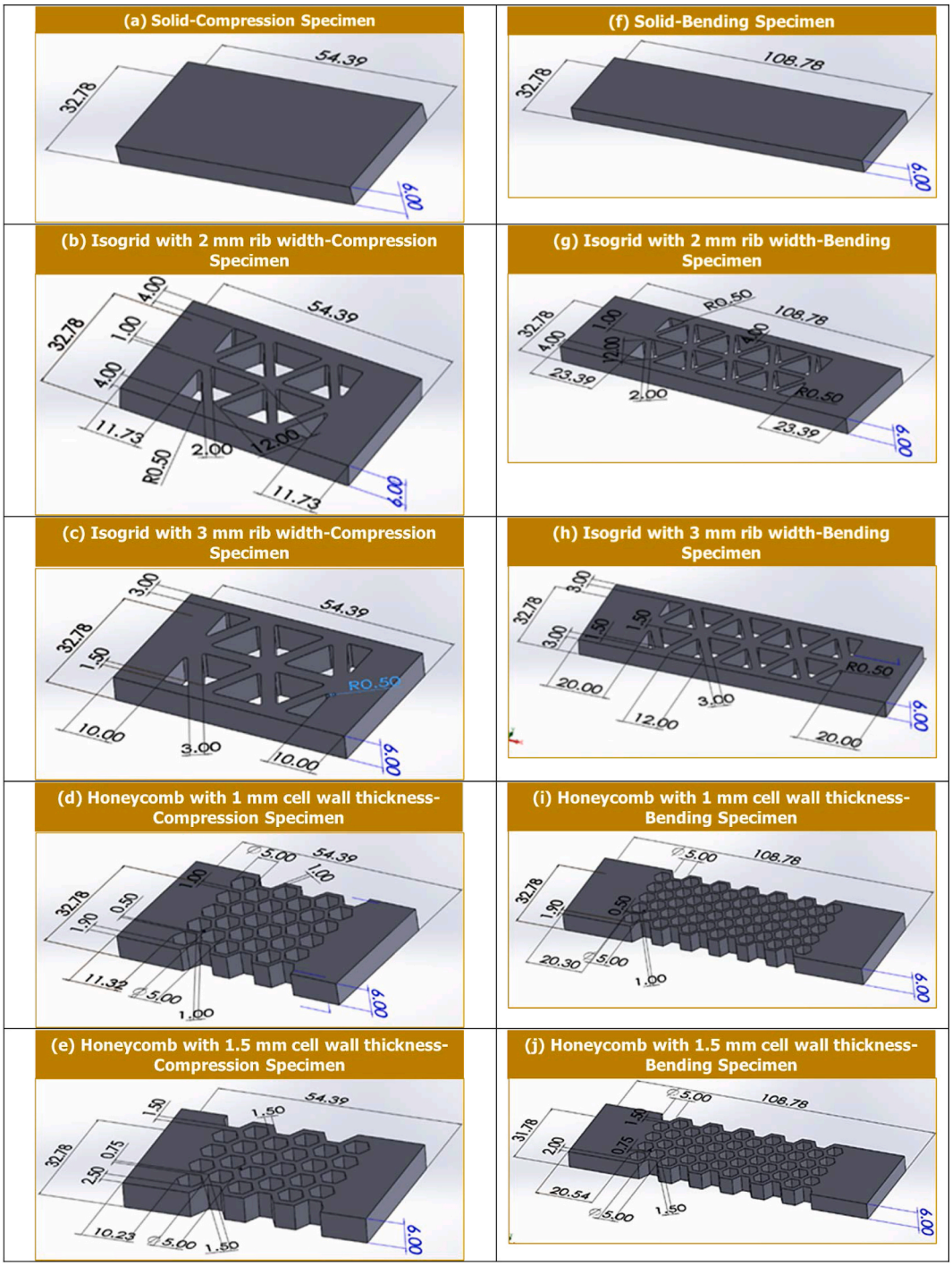

Fig. 1. Topology and geometry of specimens for compression (a–e) and bending/modal (f–j) testing, (Unit: mm).

utilizing the best design was modeled, manufactured, assessed, and validated. Furthermore, the optimal design can be utilized in numerous other potential applications, such as machinery and transportation vehicles, requiring high stiffness- and strength-to-weight ratios.

2. Materials and methods

2.1. Material, design, and manufacturing

This study dealt with AA 7075-T0 Al-alloy, which NASA lists as one of the aerospace material grades with a 103 MPa yield tensile strength and a 228 MPa ultimate tensile strength. A 7075-T0 Al-alloy was received as plates of 6 mm thickness. Five distinct satellite wall panel designs were proposed and examined in the first part of this work. The first and second designs were isogrid structures with rib widths of 2 and 3 mm, respectively. Honeycomb structures with varied cell wall thicknesses of 1 and 1.5 mm were the third and fourth designs, respectively. A solid wall panel is used as the fifth configuration for comparison. The topology and geometry of the different designs are shown in Fig. 1(a–j). These different testing specimens were machined from the as-received plates using CNC laser cutting.

2.2. Modal testing

The objective of performing a modal analysis is to identify a system's inherent dynamic characteristics, such as natural frequencies and mode shapes, and then use these to develop mathematical modal matrices of the system's dynamic behavior. These derived matrices from the modal analysis depend on the estimated contribution of the mass, stiffness, and damping characteristics in the modes of concern at specific boundary conditions that the structure is experiencing. It involves detecting the reaction time and impulse time signals, applying the fast Fourier transform, and calculating the frequency response function. A modal analysis determines the frequency at which the structure will completely absorb the energy delivered to it as well as the shape that corresponds to this frequency [21]. To ensure that they are far from the excitation frequencies and prevent resonance failure, a designer must be aware of a system's inherent vibration frequencies. To better comprehend how structures behave dynamically and to maximize their dynamic characteristics, modal analysis is required.

In the current work, evaluating the dynamic behavior of the different designs of the wall panel structures through a modal analysis using the Ansys workbench was performed to determine the natural frequency and the mode shape for ten modes of vibration. The model was solved for total deformation, which implies that the equations calculating the total deformation from the numerical analysis module will be solved by the Ansys simulation solver. The goal of this is to identify the optimal design with the least amount of distortion. Moreover, an experimental vibration (modal) test was conducted for validation of the dynamic behavior resulting from the FEA.

For the experimental vibration test, an electrical vibrator with a sharp end was utilized as an exciter to apply a known input force to the specimens; a cast-iron vise was used as a fixing mechanism; a headset sensor was employed as a transducer to transform the physical motion of the structure into an electrical signal; a headset amplifier was adopted as a signal conditioner amplifier to make the transducer properties compatible with the digital data acquisition system's input circuitry; and a desktop computer with Multi-Instrument Pro by Virtins software was employed to carry out modal analysis and signal processing operations. Experimental tests were performed on the bending specimens of the different designs (Fig. 1(f–j)) before the bending test. The specimen was fixed in the vise and rigidly held with a layer of leather and a piece of foam for more noise cancellation, then the excitation was applied by the electrical vibrator. The transducer was connected to the computer and verified. The results were monitored on the computer screen and recorded as amplitude-frequency graphs. Testing for frequency is done in a free-standing mode. Each sample is subjected to a frequency test multiple times, with the final frequency being the average of the many frequencies detected.

2.3. Mechanical testing

Finite element analysis (FEA) with the Ansys workbench was used to simulate compression and bending testing for the different designs to study the effects of the different designs on the mechanical performance. The specimens used for compression testing were $54.39 \times 32.75 \times 6$ mm (Fig. 1(a–e)), while those used for bending tests were $108.75 \times 32.75 \times 6$ mm (Fig. 1(f–j)). The explicit dynamic analysis was used to simulate the compression test in one step, using an end time of 0.0005 s and a displacement of -18 mm. Static structural analysis was used to simulate the bending test. A three-point bending flexural test was adopted in FEA. Three cylinders, i.e., pinballs, of 2 mm radius were used for conducting the test and fixing the specimen. One cylinder touches the bending specimen in the middle of the upper face, which was used to apply the bending load. The other two cylinders fix the specimen at the lower face ends. In this simulation, three contact regions between the three fixing cylinders and the specimen should be defined. A frictional contact was defined between the mating surfaces of the upper cylinder and the center of the upper face of the specimen using a friction coefficient of 0.1. In order to simplify the model, frictionless contacts were defined between the mating surfaces of the lower cylinders and the lower face ends of the specimen. The number of steps was set to be 10, with an end time of 1 s.

For validation of the FEA results, experimental testing was conducted. Compression tests were performed using a universal testing machine at a strain rate of 2 mm/min. Load-displacement curves for all designs were derived from the compression tests. To account for stress, the average cross-sectional area was calculated for the different designs using one of the CAD programs (Fusion 360). To account for the strength-to-weight ratio, the weight of each specimen was calculated using SolidWorks and experimentally measured

using a high-accuracy digital balance for more assurance. Bending tests were conducted using a three-point bending flexural test to account for the angles of deflection at failure. The bending specimens were fixed using a vise, and a cylinder of 22 mm diameter was used as a bending tool. The experimental setup of both the compression test and the bending test is shown in Fig. 2(a, b).

2.4. Design development

The second part of this work involves studying the influence of varying the length of the sides of the grid structure that revealed the best mechanical performance, namely 12, 18, and 24 mm, on the mechanical and dynamic performance of the wall panel of 115 × 90 × 6 mm using the same modules of finite element analysis (FEA) with the Ansys workbench to achieve the lowest possible mass while keeping the structure's integrity intact. Finally, using the same finite element analysis (FEA) modules with the Ansys workbench, a modified design for the satellite wall panel with a skinned wall, i.e., an outside solid face, was introduced and evaluated. A 7075 aluminum plate with dimensions of 115 × 90 × 6 mm was CNC milled to create the grid structure, leaving a 1 mm thickness that served as the skin of the grid wall panel. By doing this, the gluing process to create an adhesive joint between the grid core and the outside skin was avoided.

2.5. Manufacturing and assessment of the satellite wall panels

2.5.1. Satellite components and assembly

After determining the grid panel structure that results in the best mechanical performance, the manufacturing of a hexagonal satellite structure prototype was carried out using the best design. All geometries have been modeled using the SolidWorks software package. Most of the dimensions in the current model have been approved by research held by a group of researchers at Virginia Polytechnic Institute, published in 2002 [2]. However, the current work first optimizes the most critical variables of the design, as discussed in an earlier part, to reach the best design that will guarantee the highest performance, integrity, and robustness of the structure.

The structural assembly consists of eight grid plates. The top and bottom end plates have been configured to be 166.14 mm for the diagonal of the hexagonal plate, with a plate thickness of 6 mm. The plate was provided with six 4 mm diameter countersunk through holes, exactly where fasteners would be fitted. The side panel was modeled to have a skinned grid design of 115 mm length, 90 mm width, and 5 mm thickness. Each panel was provided with four 6 mm-diameter holes where fasteners would be provided to connect the side panels together. Two configurations of the brackets have been modeled to bring the individual parts of the assembly together. The first configuration of the bracket with an angle of 120° was employed as a connecting element between two adjacent side panels of the satellite body. The second configuration of the bracket design with an angle of 90° was modeled for the purpose of bringing the side panels and the end plates all together. The bracket is at a right angle with an adequate fillet at the corner to prevent potential failure.

The assembled satellite prototype was then tested through a series of environmental tests to ensure the structure's ability to withstand both static and dynamic loading introduced during the launch phase. Three dynamic tests, namely static, modal, and random vibration analyses, were applied to the prototype structure using FEA to investigate the integrity and stiffness properties of the satellite assembly and its ability to survive the extreme conditions in space. An experimental modal test was conducted on the manufactured satellite prototype to validate the simulated FEA dynamic results.

2.5.2. Dynamic testing

The goal of the static analysis is to evaluate how the present proposed satellite structure responds to the mechanical environment both statically and dynamically. The satellite structure is simultaneously subjected to a quasi-static acceleration of 11 g in the X, Y, and Z directions, simulating its static reaction. It was supposed that the structure was clamped onto the rails' top and bottom surfaces. The

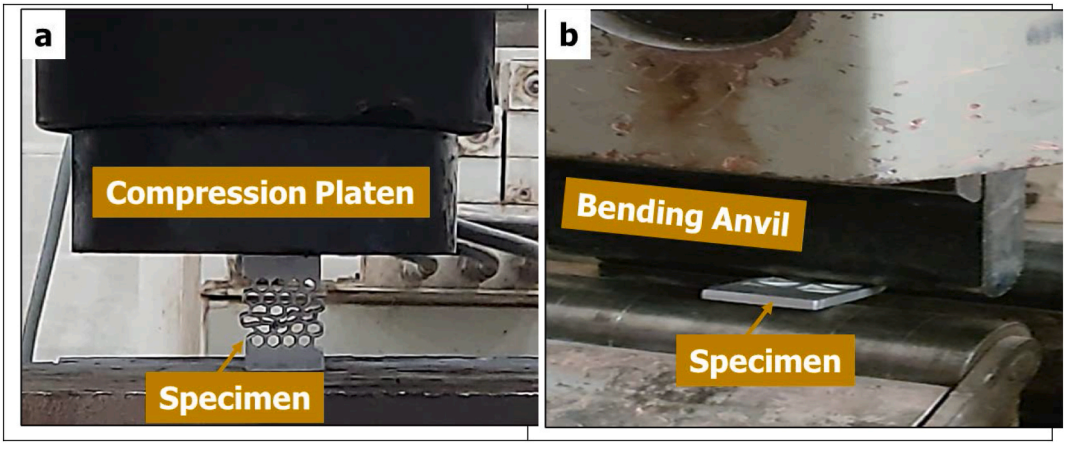

Fig. 2. Experimental setup: (a) compression test and (b) bending test.

Table 1
Equivalent von Mises stress values, modal analysis results, and experimental results of the studied designs.

Specimen	Weight of compression specimens (g)	Weight of bending specimens (g)	FEA results					Experimental results		
			Equivalent (von Mises) compression strength (MPa)	Compressive strength-to-weight ratio (MPa/g)	Equivalent (von Mises) bending strength (MPa)	Bending strength-to-weight ratio (MPa/g)	Lowest natural frequency (Hz)	Compressive strength (MPa)	Compressive strength-to-weight ratio (MPa/g)	Natural frequency (Hz)
Solid	30.06	60	738.22	24.56	1667.1	27.79	420.43	782.99	26.05	3100
Isogrid of 2 mm rib width	21.75	43	728.01	33.47	2136.5	49.69	338.95	691.03	31.77	2368
Isogrid of 3 mm rib width	21.76	43.475	720.88	33.13	2053.6	47.24	332.27	679.13	31.21	2110
Honeycomb of 1 mm cell wall thickness	17.998	33.956	354.83	19.71	1183.3	34.85	189.03	321.47	17.86	1507
Honeycomb of 1.5 mm cell wall thickness	18.745	36.65	496.66	26.49	1615.3	44.07	249.94	576.89	30.78	1808

satellite within the rocket is simulated in this situation. A static structural analysis was created utilizing the Ansys Workbench by defining the material, geometry, and connections, then solving for equivalent static von Mises stress and deformation distribution. The modal analysis was also performed on the assembled satellite prototype to determine the resonance frequencies of the geometry.

In random vibration analysis, a series of random numbers at some intervals are plotted against time. It is difficult to extract the frequency information from that using something like a Fourier analysis, as all frequencies are present in a randomly generated signal. This means that if the structure is in a situation where it is not being uniformly forced but instead has some random forcing component (quite common in rocket launches), the structure is going to respond to every single forcing frequency simultaneously, including the modes. By introducing random vibrations through the mechanical interface and vibrations produced during satellite launch, vibration analysis can verify the strength and structural durability of the satellite. These analyses confirm the workmanship of the satellite and are suitable for subsystem- or equipment-level testing. The power spectral density (PSD) of acceleration analysis, which measures the power intensity of a vibration signal in the frequency domain, is a commonly used method to determine the extent of damage caused by random vibration. The average value of all the amplitudes within a specific frequency range can be used to assess the continuously fluctuating acceleration. The average value of the acceleration at a certain frequency tends to remain relatively consistent despite the continual fluctuations [1,22].

Random vibration analysis is often carried out between 20 and 2000 Hz, which is a wide frequency range. Such a study statistically examines a structure's response to a random vibration rather than focusing on a particular frequency or amplitude at a particular point in time. The primary conclusions drawn from the investigation are whether or not the resonance is within the structure's inherent frequencies and how the structure responds overall.

The random vibration module in the Ansys Workbench was used in the current analysis. Boundary conditions, i.e., the way to quantify this interval of forcing amplitudes (the range of random numbers), are Power Spectral Density (PSD). This can be given in terms of acceleration, displacement, or velocity, but essentially quantifies the amount of average power present in the frequencies. In this analysis, add a "PSD G Acceleration" boundary condition, where G denotes the G-force, and set it to all fixed supports, using the same geometry and mesh as the modal analysis. The load will be supplied by the Shuttle Hichhiker Experiment Launcher System (SHELS).

A qualified vibration analysis professional from the American Vibration Institute (AVIC level 4) oversaw the implementation of the experimental modal test to validate the FEA dynamic results. An application of a free-free vibration modal test that simulates launch vehicle conditions has been implemented. The test was conducted between the frequencies of 20 Hz and 2000 Hz. The test was carried out by two channels to specify the natural frequencies using a table covered in sponge, two separate acceleration sensors, one with a rubber tip and the other with a metallic tip, and a tachometer. The sensor was initially fastened to the top panel before being moved to the side panels. The panel is then repeatedly hit with a hammer, and the results are recorded and appear on the attached screen. The frequencies with the highest peak amplitudes were the natural frequencies that were recorded.

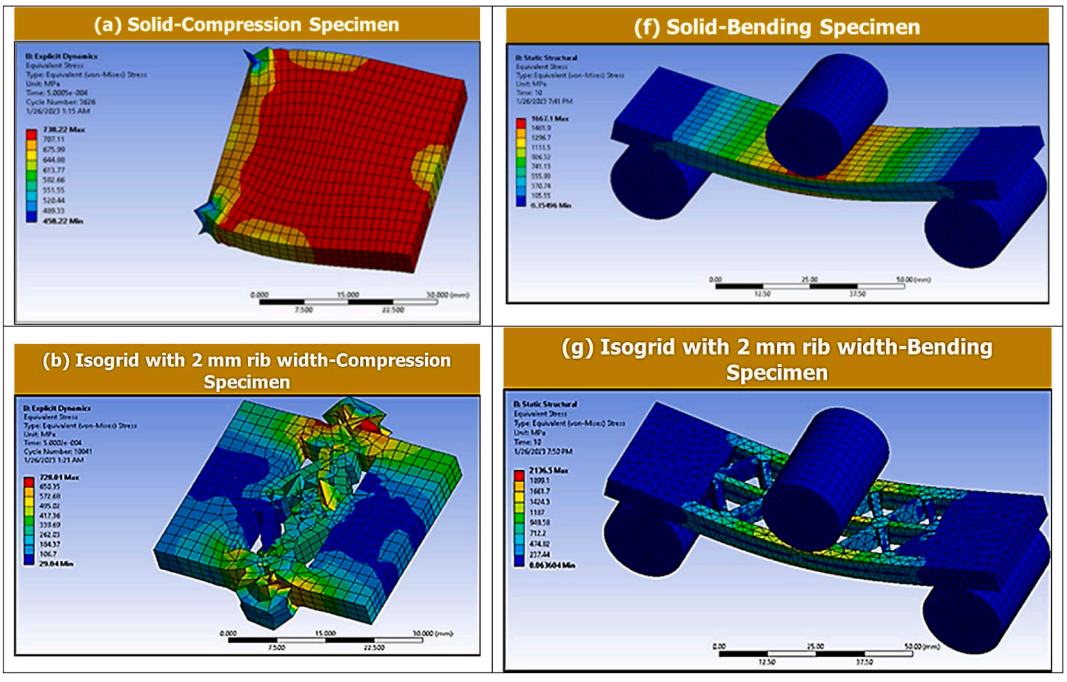

Fig. 3. Equivalent von Mises stresses FEA results for the different designs: (a,f) solid specimen, (b,g) Isogrid specimens with 2 mm rib width, (c,h) Isogrid specimens with 3 mm rib width, (d,i) Honeycomb specimens with 1 mm cell wall thickness, and (e,j) Honeycomb specimens with 1.5 mm cell wall thickness..

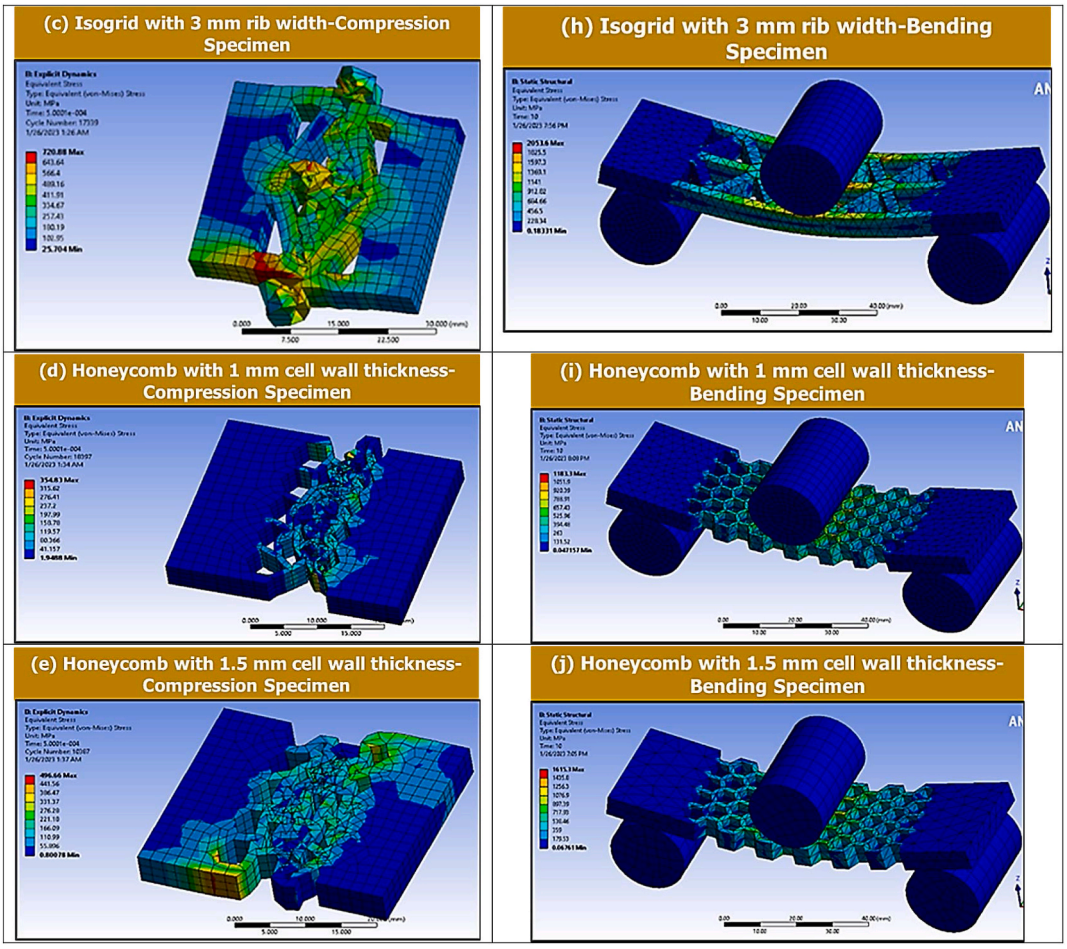

Fig. 3. (*continued*).

3. Results and discussion

3.1. Evaluation of the mechanical performance of the different wall panel designs using FEA and experimental testing

Table 1 summarizes the FEA and experimental results for the studied wall panel designs. It is evident that the FEA and experimental results agree quite well. The equivalent von Mises stresses of the compression and bending tests using Ansys workbench FEA are presented in Fig. 3(a–j). The solid specimens show the lowest values of strength-to-weight ratio in both compression and bending tests of 24.56 and 27.79 MPa/g, respectively. Isogrid configurations exhibit better mechanical performance in terms of compressive strength, bending strength, and strength-to-weight ratio compared with honeycomb configurations. For isogrid structures, reducing the rib width from 3 to 2 mm increases mechanical performance in both compression testing and bending testing by 1% and 4%, respectively (Table 1). This result is in agreement with the findings of Ciccarelli et al. [8], who studied the influence of rib width on the strength of polyamide. For honeycomb structures, increasing the cell wall thickness from 1 to 1.5 mm increases the mechanical performance in both compression and bending testing by 40% and 36.5%, respectively, as presented in Fig. 3(a–j) and Table 1.

Regarding the experimental testing, photos of the compression specimens after tests are presented in Fig. 4(a). All configurations experience local buckling failure mode as the value of rib width and cell wall thickness is slender than the wall panel thickness. This observation is in agreement with previous findings [8,9]. Fig. 5 presents the load-displacement curves of the different designs resulting from a practical compression test. As shown, the isogrid configurations reveal higher load capacity compared with honeycomb configurations. The experimental bending results are more qualitative, depending on the bending angle. The lowest bending angle reveals higher bending strength. Photos of the specimens after bending tests are arranged in a line to compare the amount of deflection, as shown in Fig. 4(b). The experimental results of the mechanical testing of the different configurations confirm and validate most of the FEA results, as presented in Table 1.

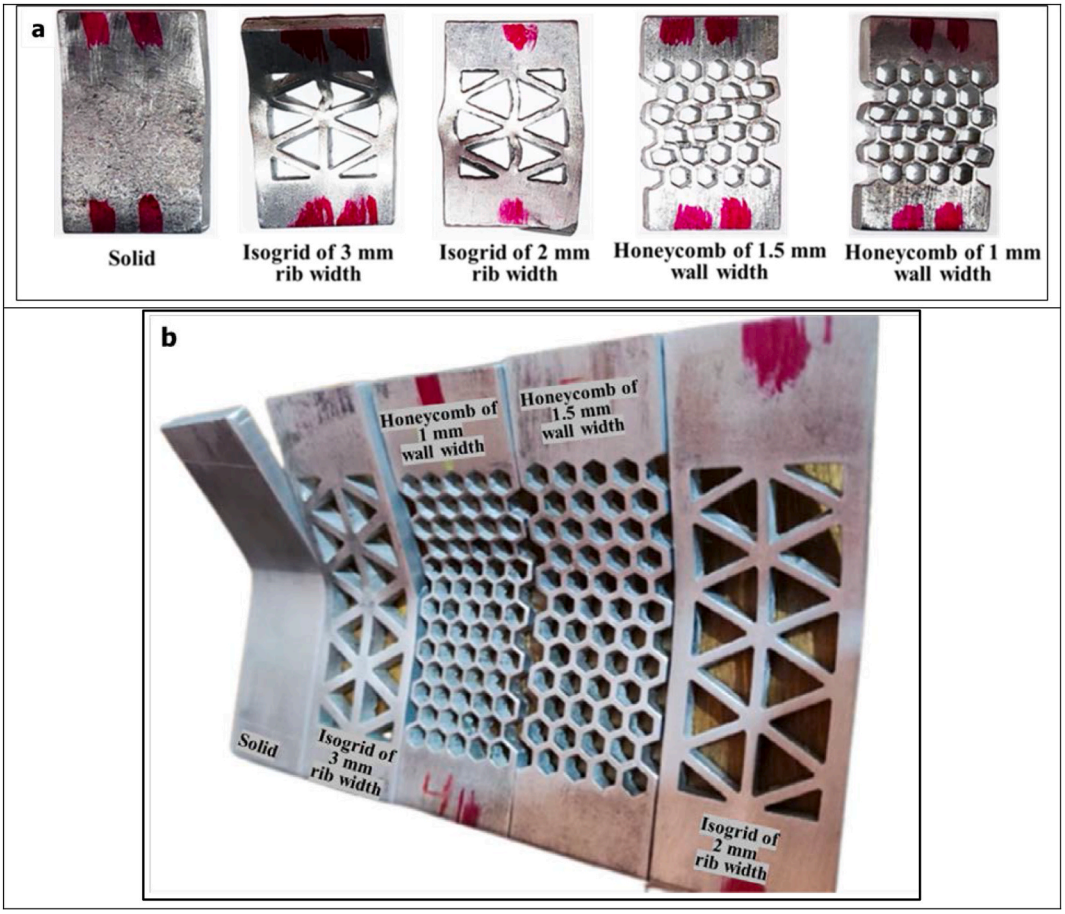

Fig. 4. The specimens after experimental testing: (a) compression failures and (b) bending failures.

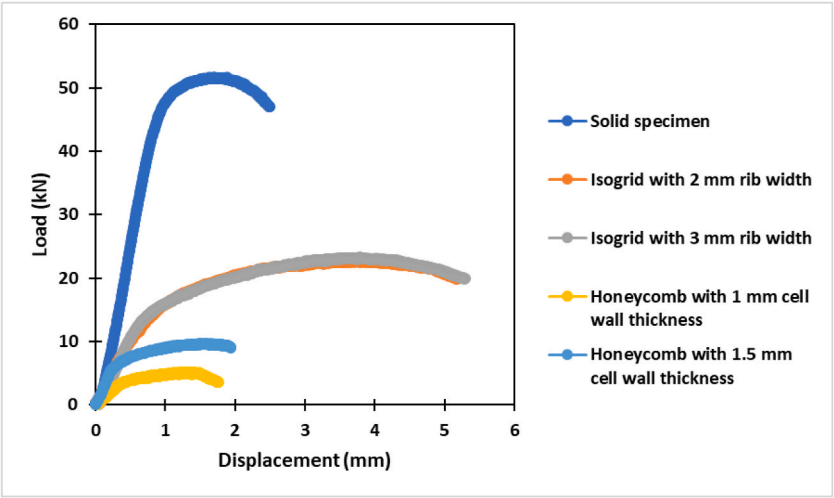

Fig. 5. Load-displacement curves of the different designs resulted from compression test.

3.2. Evaluation of the dynamic behavior of the different wall panel designs using FEA and experimental testing

The dynamic characteristics of a structure are examined in the frequency domain by modal analysis. Any system, equipment, or structure that is excited will show a strong peak in response at resonance when the forcing frequency is equal to the system's inherent frequency. In order to prevent the structure from collapsing due to resonance, modal analysis determines the different periods at which a structure will naturally be resonant. Modal analysis also provides the boundary conditions for the subsequent vibration analysis. For satellites, the natural frequency must be higher than 50 Hz to avoid resonance [1,2]. Moreover, modal analysis generates related mode shapes or deformed shapes at each natural frequency. The natural frequencies at the various modes of the FE modal analysis are presented in Fig. 6(a–e). The total deformation and specimen mode shapes of mode 1 of the modal analysis for the different designs are shown in Fig. 7(a–e).

The isogrid configurations exhibit better dynamic vibration behavior than honeycomb configurations, i.e., a higher natural frequency. Reducing the rib width of the isogrid structure from 3 mm to 2 mm enhances the dynamic vibration behavior by increasing the natural frequency from 332.27 to 338.95 Hz as the weight of the wall panel decreases. Dawood et al. [12] found the same behavior. For honeycomb configurations, increasing the cell wall thickness from 1 mm to 1.5 mm promotes dynamic vibration behavior by raising the natural frequency from 189.03 to 249.94 Hz. This result agrees with previous work by Sadiq et al. [16], who studied the influence of the honeycomb variables on the forced vibration behavior of sandwich panels with honeycomb cores. Mansour et al. [20] reported similar behavior. In the case of honeycomb configurations, increasing the weight of the wall panel increases the natural frequency. This is attributed to the fact that the mass rise was not the dominant factor affecting the natural frequency since the stiffness of the wall panel structure was also changed due to the variation in the value of the second moment of inertia for each design [12].

The honeycomb structure with a cell wall thickness of 1 mm reveals the minimum value of the natural frequency of 1507 Hz, while the isogrid structure with a rib width of 2 mm exhibits the maximum value of the natural frequency of 2368 Hz (Table 1). All the studied designs satisfy the criteria for the dynamic vibration of satellites and can avoid failure due to resonance, as their natural frequencies exceed 100 Hz.

The amplitude-frequency responses for the different grid configurations of the experimental modal test are presented in Fig. 8(a–e). The simulated and experimental results show the same behavior but with large differences in values. This is due to the fact that the modal test of the FEA used free vibration, whereas forced vibration was undertaken in the experimental modal test.

3.3. Influence of the length of the sides of the isogrid structure on the mechanical and dynamic performance

The above results suggest the isogrid structure with a 2 mm rib width is the best candidate for manufacturing the satellite wall panel. Providing the grid array with skins has been an effective way of increasing the overall structural stiffness. A 12 mm length of the sides was undertaken in the above study. In this part, the effect of the length of the sides, namely 12, 18, and 24 mm, of this isogrid

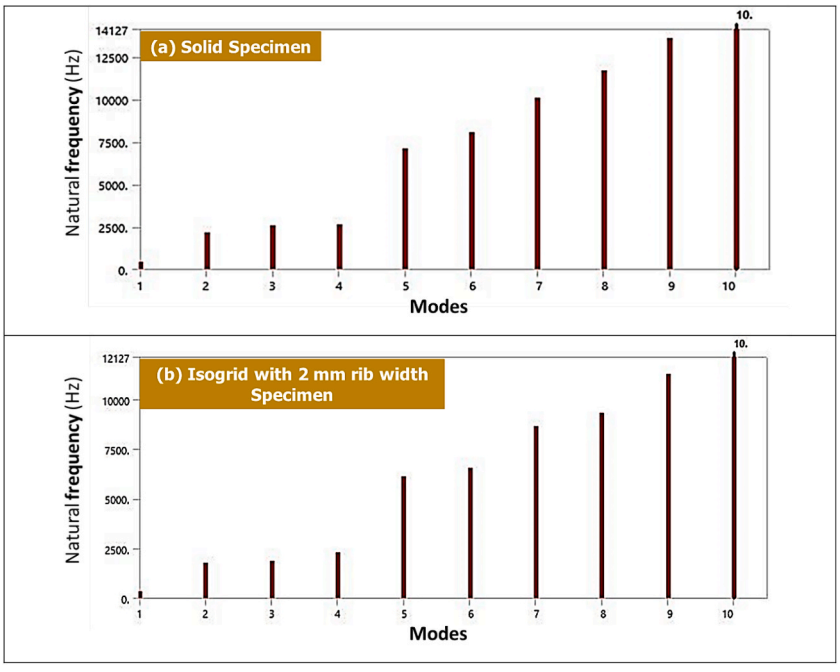

Fig. 6. The natural frequencies at the different modes of the FE modal analysis: (a) solid specimen, (b) Isogrid specimens with 2 mm rib width, (c) Isogrid specimens with 3 mm rib width, (d) Honeycomb specimens with 1 mm cell wall thickness, and (e) Honeycomb specimens with 1.5 mm cell wall thickness.

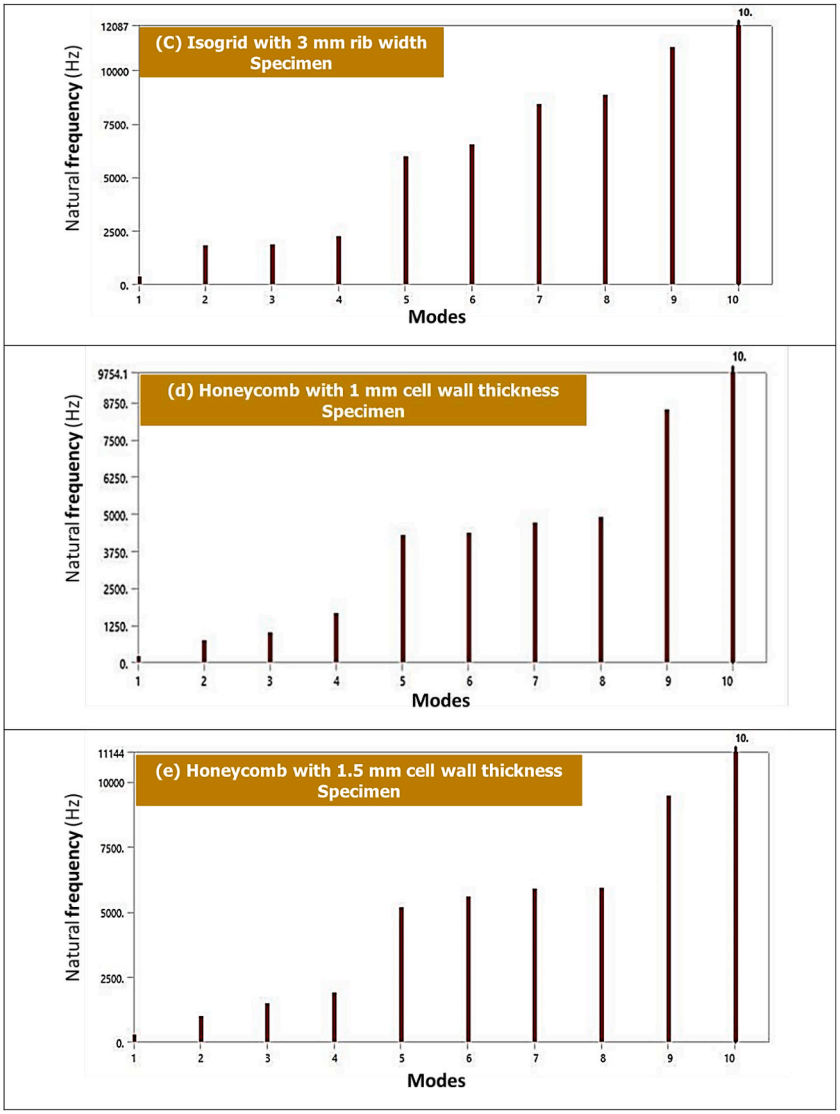

Fig. 6. (*continued*).

configuration was studied on the mechanical and dynamic behavior of the wall panel of 115 × 90 × 6 mm. The equivalent von Mises stresses of the compression and bending tests using Ansys workbench FEA are presented in Fig. 9(a–f). The wall panel of 12 mm length of the sides exhibits local buckling modes of failure in compression. The wall panels of 18 mm and 24 mm length on the sides show rib rippling in addition to the local buckling due to the large rib spacing. Table 2 summarizes the FEA results for the isogrid wall panel with a 2 mm rib width at different lengths of the sides. By increasing the length of the sides of the isogrid structure from 12 mm to 24 mm, the weight of the wall panel decreases from 102.02 g to 66.379 g. Increasing the length of the sides promotes the strength of the wall panel and strength-to-weight ratio in both compression and bending while decreasing the natural frequencies from 1241.5 Hz to 1031.1 Hz, which is still safe as it is sufficiently higher than the critical limit of the natural frequency of satellites (50 Hz).

3.4. A modified design for the satellite wall panel

The grid structure geometry is anisotropic, and the longitudinal direction reveals higher stiffness [7]. Nevertheless, the core behaves nearly isotopically for in-plane loads when assembled in a sandwich configuration. Unfortunately, sandwich structures are susceptible to collapse due to the heterogeneous character of the core/skin sheet assembly, which results in significant localized stress concentrations at the adhesive layers utilized in assembly [15].

A modified design for the satellite wall panel was introduced and tested using the same modules of finite element analysis (FEA) with the Ansys workbench. This modified design is a skinned wall panel, i.e., an isogrid structure panel with an outer solid face, or skin. This skinned wall panel was produced by CNC milling a 115 × 90 × 6 mm wall panel and leaving a 1 mm thickness to act as the skin of a

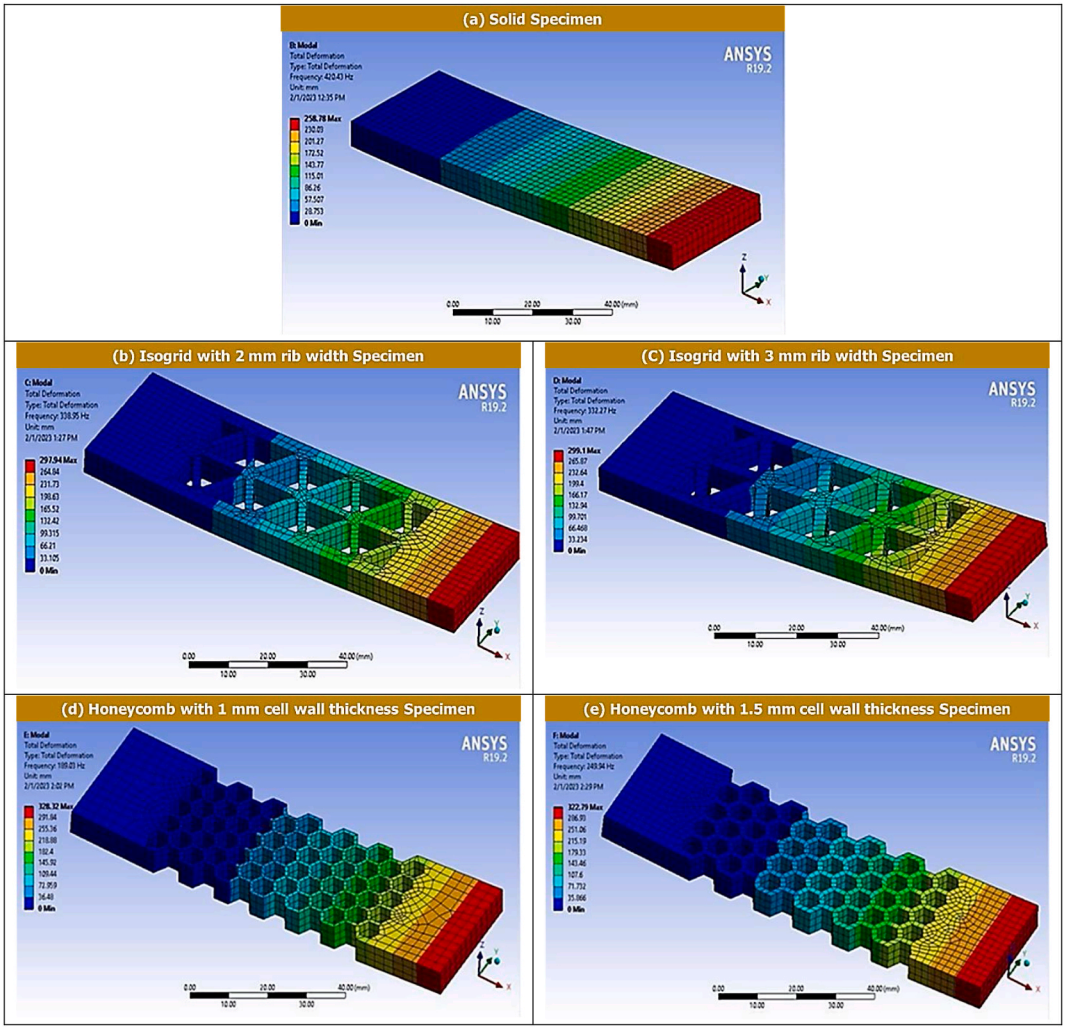

Fig. 7. Total deformation and specimen mode shapes of mode 1 of the modal analysis for the different designs: (a) solid specimen, (b) Isogrid specimens with 2 mm rib width, (c) Isogrid specimens with 3 mm rib width, (d) Honeycomb specimens with 1 mm cell wall thickness, and (e) Honeycomb specimens with 1.5 mm cell wall thickness.

sandwich panel, avoiding the process of gluing and the drawbacks of the adhesive joint between the isogrid panel and the outer skin. The skinned wall panel was selected to have 24 mm length of sides. The geometry of the open and skinned isogrid wall panels with a 2 mm rib width and a 24 mm length of sides is presented in Fig. 10(a, b). Equivalent von Mises stress FEA results for the skinned isogrid panel with a 2 mm rib width in compression and bending are shown in Fig. 11(a, b). The skinned isogrid panel reveals a strength of 725.13 MPa in compression and 2666.9 MPa in bending. The skinned panel exhibits a local buckling mode of failure with rib rippling, as skin restraint cannot stop these long ribs from becoming rippled. A similar observation was reported by Li et al. [10].

The skinned wall panel reveals a slight improvement in compression strength as compared to a wall panel with a 24 mm length of sides and a moderate strength in bending between the open isogrid configurations of 18 mm and 24 mm length of sides. Using this modified skinned wall panel, dynamic behavior is significantly promoted, as the natural frequency increases to 1308.7 Hz, as compared with the open isogrid configurations of 18 mm and 24 mm length of sides. Moreover, better dynamic behavior is expected as compared with employing the open isogrid structure of the same length of sides with separated skin due to the avoidance of an adhesion joint between the two panels.

3.5. Dynamic performance of the assembled satellite

Based on the above analysis, the best structural design selected for satellite wall panels is the skinned isogrid design with a 2 mm rib width and a 24 mm length of sides. An array of equal-length triangle cutouts is used in this design to improve a flat sheet of material's structural performance. The triangle cutouts have been filleted with a rounded 0.75 mm radius fillet to avoid sharp edges and, consequently, the potential local failure of the ribs. In comparison to a solid structure, machining an isogrid pattern ideally results in a

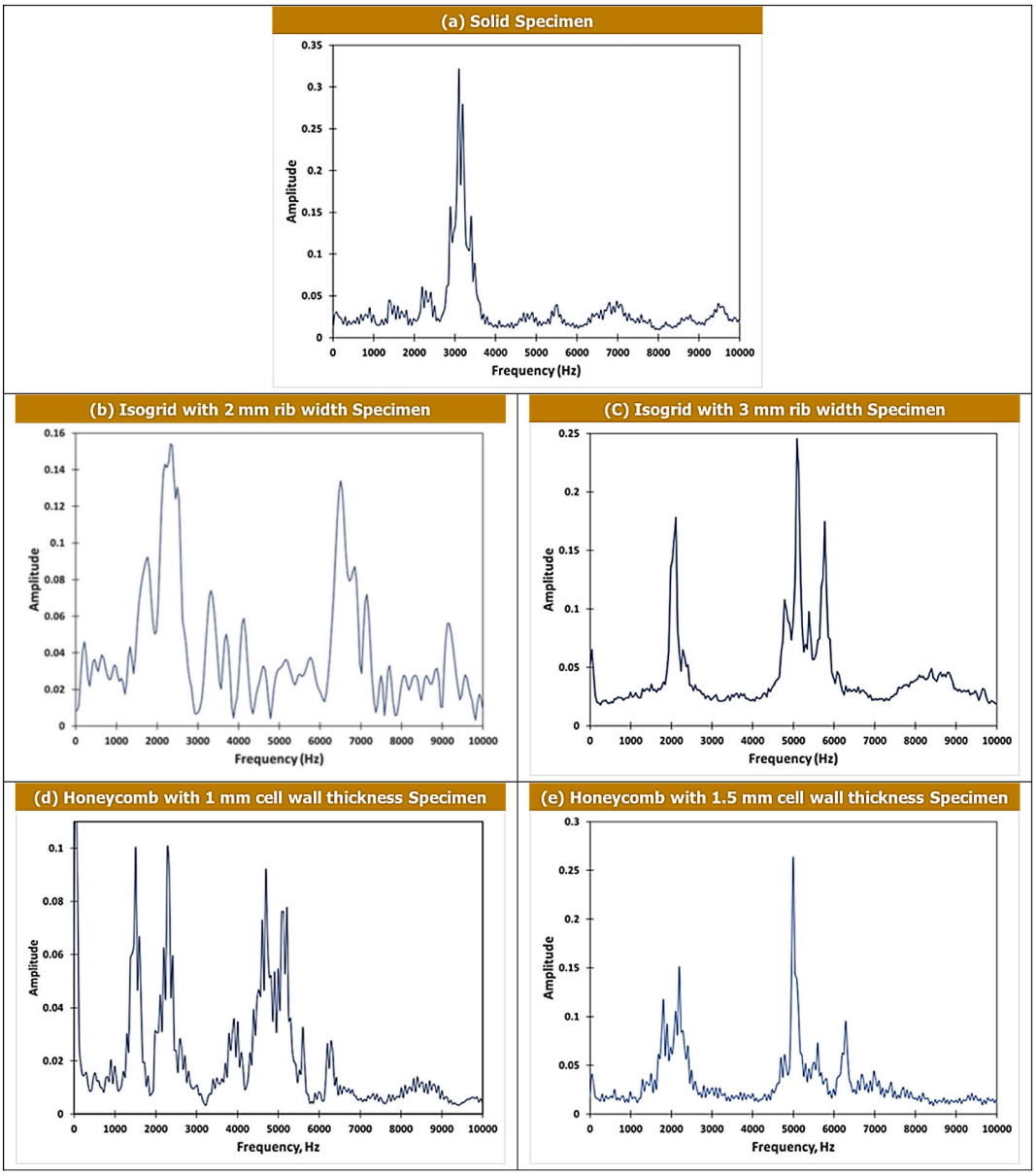

Fig. 8. Amplitude-frequency responses for the different grid configuration designs: (a) solid specimen, (b) Isogrid specimens with 2 mm rib width, (c) Isogrid specimens with 3 mm rib width, (d) Honeycomb specimens with 1 mm cell wall thickness, and (e) Honeycomb specimens with 1.5 mm cell wall thickness.

75% reduction in the original plate's mass and a 25% decrease in the plate's strength. In comparison to a solid structure, this leads to a nominal 200% gain in structural dynamic efficiency. Machining the triangle array has the additional benefit of maintaining the plate's isotropy. As a result, it shows comparable strength in all directions and has a reduced amount of concentrated stress.

After the manufacturing of all the panels involved, assembly was done. The manufactured panels are six side panels, a top panel, a bottom panel, six side angles with 120°, and twelve top and bottom angles with 90°, as shown in Fig. 12. For assembly, the first step is to bring the six panels together using 120° angles with rivet nuts and flat-head screw bolts. The second step is to join the side panels with the bottom and top panels using 90° angles by means of rivet nuts and flat-head screw bolts.

The distributions of equivalent stress and total deformation for the satellite structure of static analysis are displayed in Fig. 13. The satellite structure exhibits a maximum stress of 89.431 MPa (Fig. 13(a)), which is safe in terms of yielding in comparison to the aluminum alloy 7075-T0's yield value of 103 MPa. Fig. 13(b) shows that the structure responds with a maximum overall deflection value of 0.0134 mm, which is determined to be quite acceptable in terms of the interference caused by static deflection from the various satellite components and found to be very small in comparison to the satellite dimensions. Therefore, this hexagonal satellite

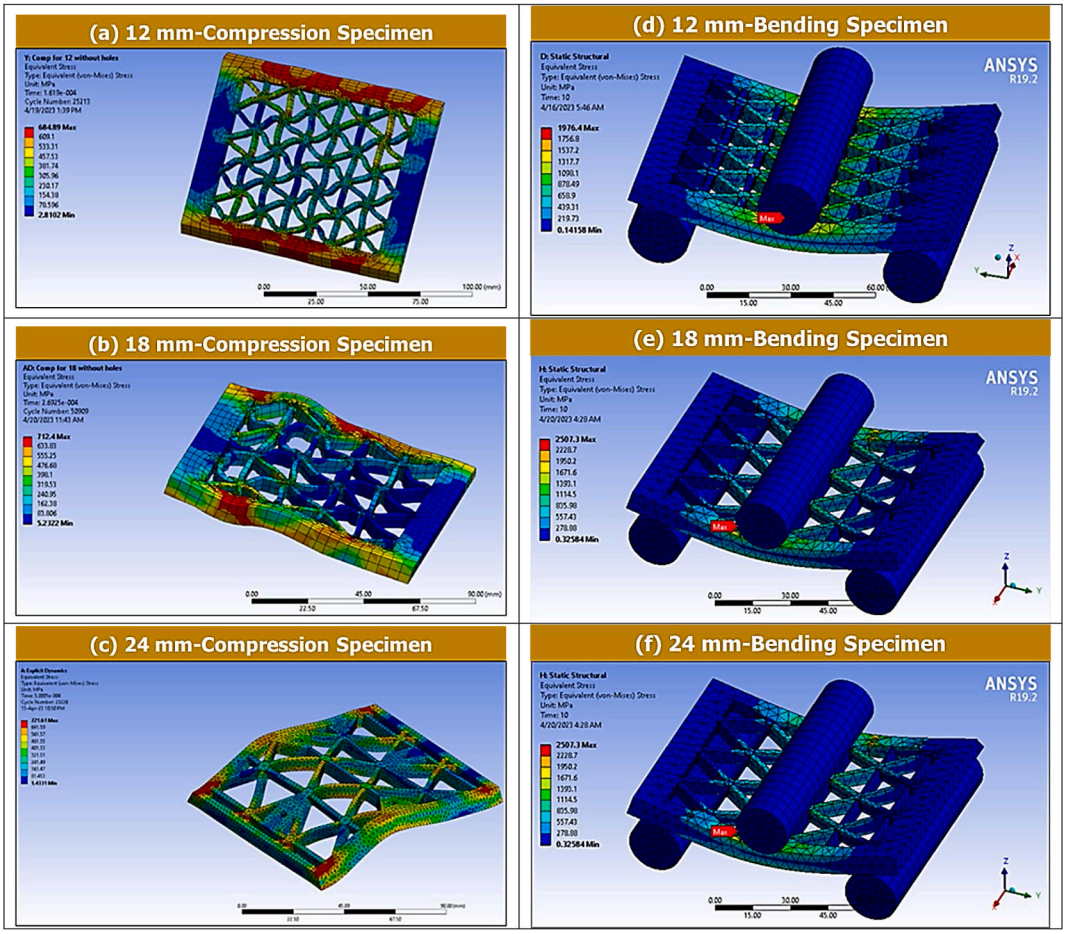

Fig. 9. Equivalent von Mises stresses FEA results at different length of sides of the isogrid structure with 2 mm rib width: (a,d) 12 mm, (b,e) 18 mm, and (c,f) 24 mm.

Table 2
Equivalent von Mises stress values and modal analysis results at different length of the sides of the isogrid panel of 2 mm rib width.

Length of the sides (mm)	Weight (g)	FEA results				
		Equivalent (von Mises) compressive strength (MPa)	Compressive strength-to-weight ratio (MPa/g)	Equivalent (von Mises) bending strength (MPa)	Bending strength-to-weight ratio (MPa/g)	Lowest natural frequency (Hz)
12	102.02	684.89	6.71	1976.4	19.37	1241.5
18	91.057	712.4	7.82	2507.3	27.54	1131.5
24	66.379	721.61	10.87	3018.6	45.47	1031.1
24 (Skinned panel)	91.341	725.13	7.94	2666.9	29.197	1308.7

assembly can withstand the launch's static loading without failure. According to the finite element study, there is a substantial margin of safety and sufficient survivability when it comes to the imposed failure modes and the worst-case static loading of applying 11 g in the three directional axes concurrently.

According to the launch vehicle's user guide (Shuttle Hichhiker Experiment Launcher System (SHELS)), the natural frequencies of the satellite should not be lower than 50 Hz. Fig. 14 exhibits the variation of frequency for the hexagonal satellite versus the number of modes. At 300.85 Hz, there is the first mode of natural frequency. The calculated number is significantly higher than the 50 Hz minimum launch load requirement. It follows that the structure won't resonate with the launch vehicle interface and won't distort during the launch. For the current satellite design, this model can therefore be regarded as safe. Fig. 15 depicts the deformation brought on by the first mode of vibration.

Random vibration analysis had been carried out over the model three times to account for all possible excitation orientations that

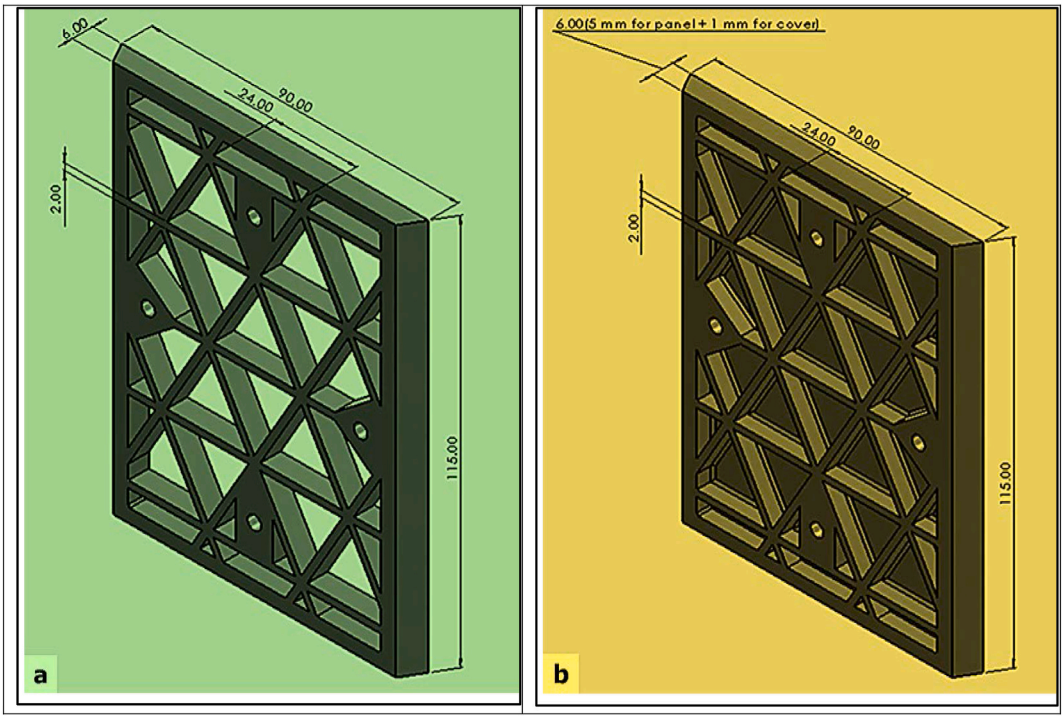

Fig. 10. Geometry of Isogrid wall panels with 2 mm rib width and 24 mm length of sides: (a) open isogrid panel, and (b) skinned panel.

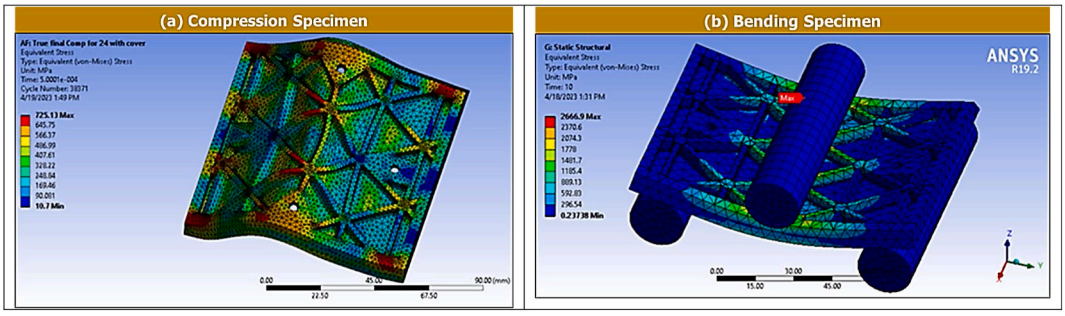

Fig. 11. Equivalent von Mises stresses FEA results for the isogrid structure with 2 mm rib width skinned panel: (a) compression test result, and (b) bending test result.

the satellite would experience in its operational stage. The following results sum up the body's response to the random vibration applied to it on the X, Y, and Z axes separately. However, the directional deformation in each case was evaluated along the three directional axes to be able to demonstrate the worst-case situation. In the first case of applying the random vibration along the X axis, the results demonstrated that the deformation along the X, Y, and Z directions was sufficiently negligible. The highest maximum deformation occurred, as expected, in the X direction. The acceleration spectral density (ASD) utilized in the ION-F random vibration test is shown in Fig. 16. Fig. 17(a–d) shows the deformation distribution for all directions when the acceleration is applied to the X axis. In the worst-case situation, the X axis loading is identified, but the 0.95 MPa maximum stress (Fig. 17(d)) is still an acceptable value, keeping attention to the structure's overall stiffness and durability. For the second case of applying the random vibration along the y-axis, the results demonstrated that the deformation along the X, Y, and Z directions was similarly safe. The highest maximum deformation occurred, as expected, in the Y direction. Fig. 18(a–d) shows the deformation distribution for all directions when the acceleration is applied to the Y axis. In a worst-case situation, the Y Axis loading is identified, but still, the 3.7 MPa maximum stress (Fig. 18(d)) is an acceptable value. For the third case of applying the random vibration along the Z axis, the results demonstrated that the deformation along the X, Y, and Z directions was all accepted. The highest maximum deformation occurred, as expected, in the Z direction. Fig. 19(a–d) shows the deformation distribution for all directions when the acceleration is applied to the Z axis. In a worst-case situation, the Z Axis loading is identified, but still, the 1.13 MPa maximum stress (Fig. 19(d)) is an acceptable value. Considering the three cases stated above, taking into account the strength of the 7075 Al-alloy, the results show that the stresses for the three

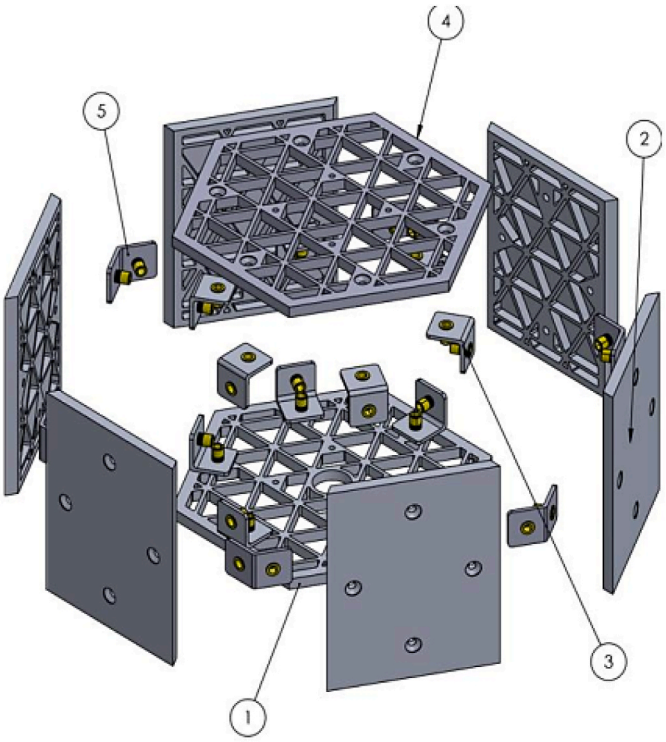

ITEM NO.	PART NAME	QTY.
1	Bottom	1
2	Face with cover	6
3	Corner with rivet nut	12
4	Top	1
5	Corner 120 with rivet nut	6
6	M4X0.8X15 SET SCREW	36

Fig. 12. The satellite assembly.

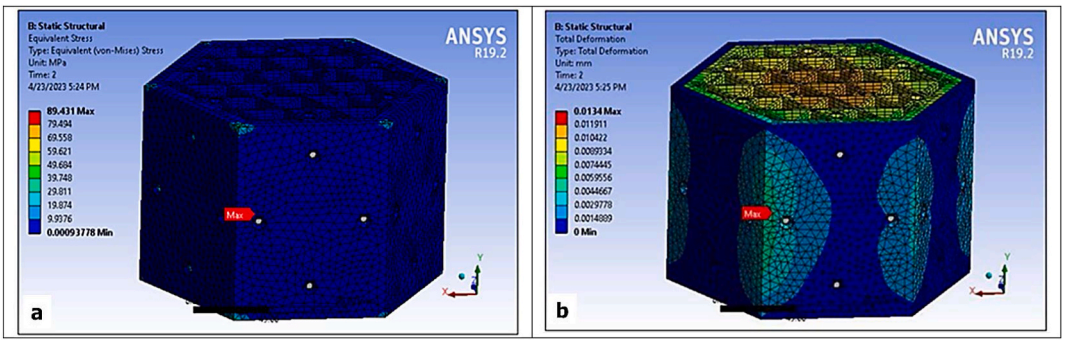

Fig. 13. Equivalent static von Mises stress of FEA results (a) and deformation distribution (b) for the assembled satellite with skinned isogrid structure from static analysis.

loading situations are quite low and within the allowed limits.

The experimental vibration test setup for satellite structure and the first mode shape result are presented in Fig. 20(a, b). In the experimental vibration test, the sensor with the metallic tip read 312 Hz on the top panel as the first mode. The results listed above demonstrated that the simulation conducted using Ansys software (300.85 Hz) was valid with a 4% error. The result of the experimental test proves that the satellite design is safe and has the capability to fulfil the requirements of the specified launcher.

4. Conclusions

It is essential to determine the best wall panel structural design that can withstand the various stress conditions that the satellite is subjected to while maintaining a low weight. The primary challenge in the present study is choosing the optimal design for the satellite wall panel. The mechanical and dynamic behaviors of five distinct designs for the satellite wall panel were investigated in the first section of the study using FEA with an Ansys workbench and experimental work. These designs were: (1) an isogrid structure with a rib width of 2 mm; (2) an isogrid structure with a rib width of 3 mm; (3) a honeycomb structure with a cell wall thickness of 1 mm; (4) a honeycomb structure with a cell wall thickness of 1.5 mm; and (5) a solid structure for comparison. The second part of this work

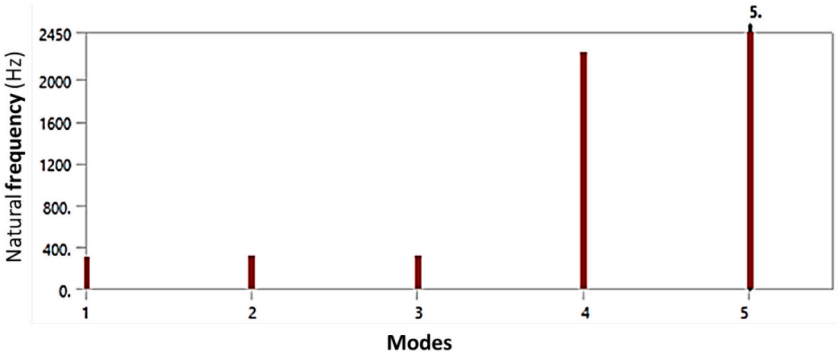

Fig. 14. Variation of number of modes vs the natural frequency for the hexagonal satellite assembly.

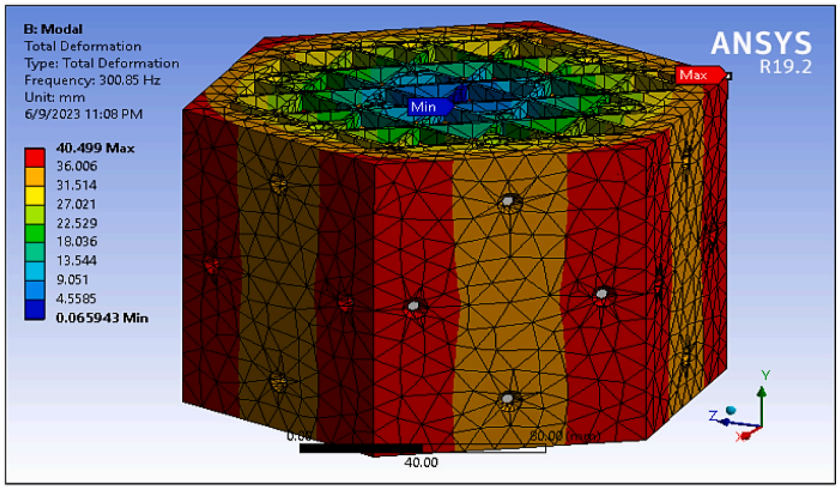

Fig. 15. Total deformation of the first mode of modal analysis.

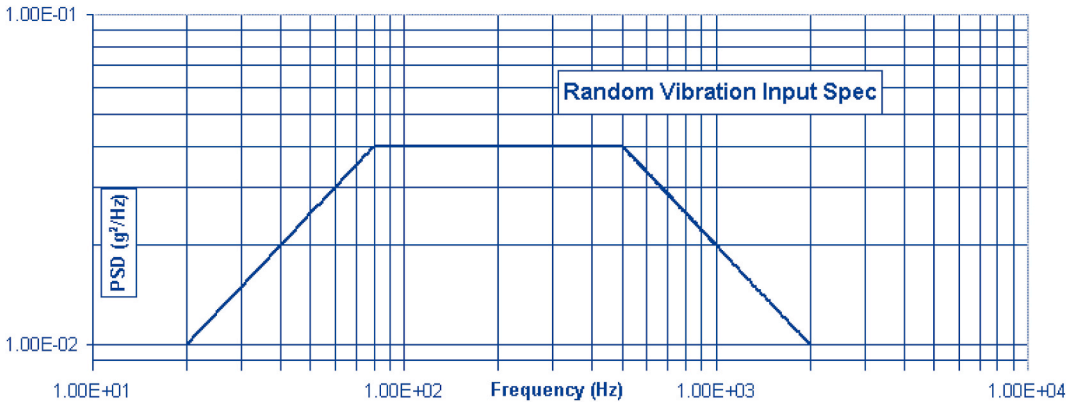

Fig. 16. Random vibrational spectrum requirements.

focuses on further design refinement using the same modules of the Finite Element Analysis (FEA) to get the best mechanical and dynamic performances. The following findings can be drawn:

1. The FEA results were verified using experimental testing.
2. Isogrid configurations exhibit outstanding mechanical and dynamic performance over honeycomb configurations.

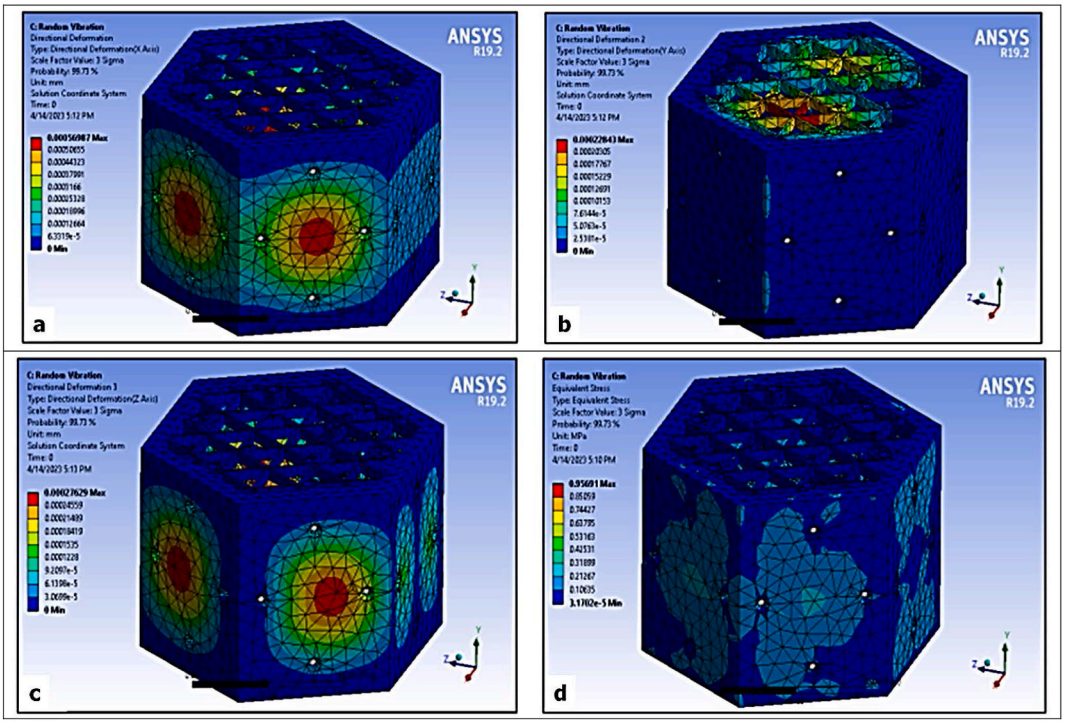

Fig. 17. Max deformation in 3 directions with applied the acceleration in X axis: (a) max deformation in X direction with applied the acceleration in X axis, (b) max deformation in Y direction with applied the acceleration in X axis, (c) max deformation in Z direction with applied the acceleration in X axis, (d) max von misses stress with applied the acceleration in X axis.

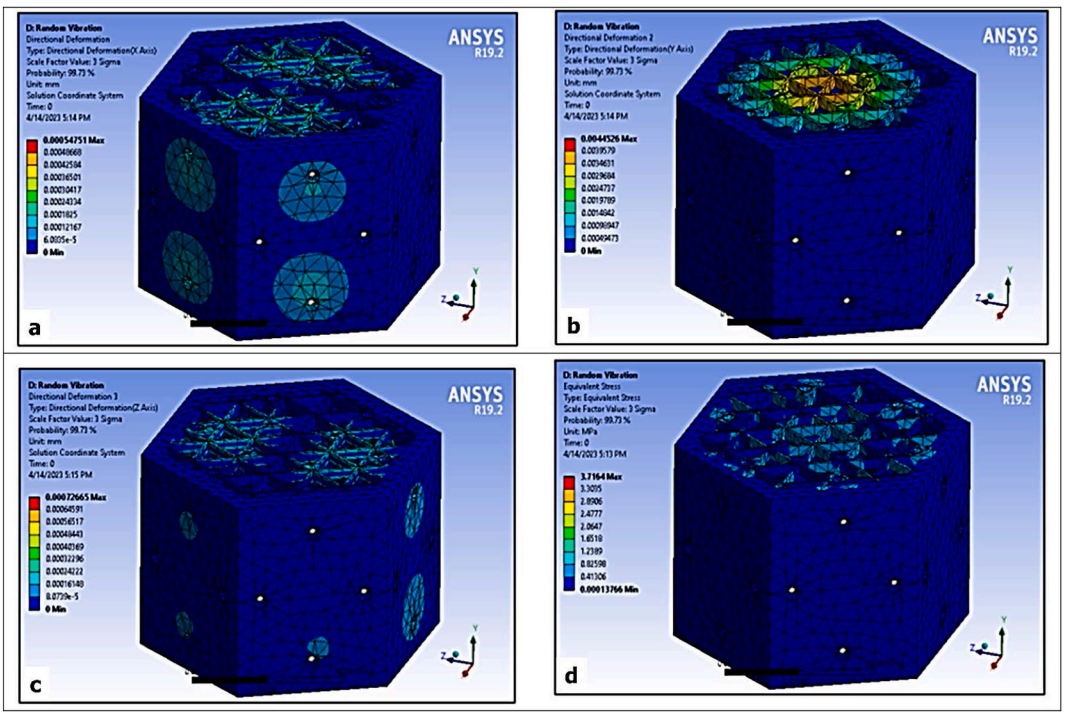

Fig. 18. Max deformation in 3 directions with applied the acceleration in Y axis: (a) max deformation in X direction with applied the acceleration in Y axis, (b) max deformation in Y direction with applied the acceleration in Y axis, (c) max deformation in Z direction with applied the acceleration in Y axis, (d) max von misses stress with applied the acceleration in Y axis.

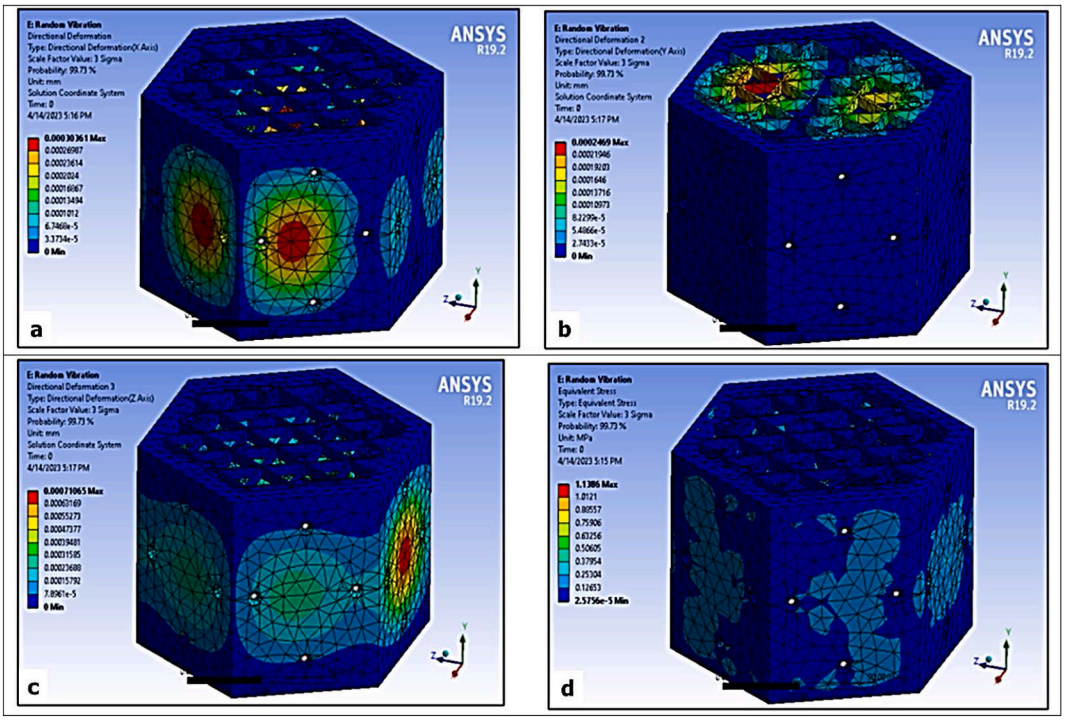

Fig. 19. Max deformation in 3 directions with applied the acceleration in z axis: (a) max deformation in X direction with applied the acceleration in Z axis, (b) max deformation in Y direction with applied the acceleration in Z axis, (c) max deformation in Z direction with applied the acceleration in Z axis, (d) max von misses stress with applied the acceleration in Z axis.

3. Decreasing the rib width for the isogrid structure from 3 to 2 mm and increasing the cell wall thickness from 1 to 1.5 mm for the honeycomb structure promote both mechanical performance and dynamic vibration behavior.
4. An isogrid structure with a lower rib thickness of 2 mm is the best candidate for a satellite wall panel because it shows the highest strength-to-weight ratio in both compression and bending testing of 33.47 MPa/g and 49.69 MPa/g, respectively, and the highest value of natural frequencies of 2368 Hz among the studied grid configurations.
5. Increasing the length of the sides from 12 mm to 24 mm promotes mechanical behavior in terms of the high strength-to-weight ratio of the wall panel and adversely affects the dynamic behavior in terms of the natural frequency.
6. The mechanical performance of the skinned wall panel with an isogrid structure of 2 mm rib width and 24 mm length of sides is comparable to the studied designs of the isogrid structure with 2 mm rib width, while the dynamic behavior was promoted as compared with the open isogrid configurations.

Finally, a hexagonal satellite structure prototype was CAD-modeled and manufactured utilizing the best wall panel design, a skinned isogrid structure with 24 mm-long sides and a 2 mm rib width. After the hexagonal satellite assembly was assessed using different FEA vibration modules, the manufactured hexagonal satellite prototype was experimentally tested using a modal test. The accuracy of the validation of the simulation and experiment results was just 4% inaccuracy. Modal analysis shows that the lowest mode is between 300 and 312 Hz, well below the critical 50 Hz threshold established by SHELS, suggesting that the manufactured satellite prototype is safe.

Data availability statement

Data will be available on request.

CRediT authorship contribution statement

Reham Reda: Writing - review & editing, Project administration, Conceptualization. **Yasmeen Ahmed:** Writing - original draft, Validation, Software. **Islam Magdy:** Software, Methodology. **Hossam Nabil:** Validation, Software. **Mennatullah Khamis:** Software, Methodology. **Mohamed Abo Lila:** Software, Investigation. **Ahmed Refaey:** Methodology, Investigation. **Nada Eldabaa:** Writing - original draft, Methodology. **Manar Abo Elmagd:** Writing - original draft, Methodology. **Adham E. Ragab:** Supervision, Funding acquisition, Conceptualization. **Ahmed Elsayed:** Validation, Conceptualization.

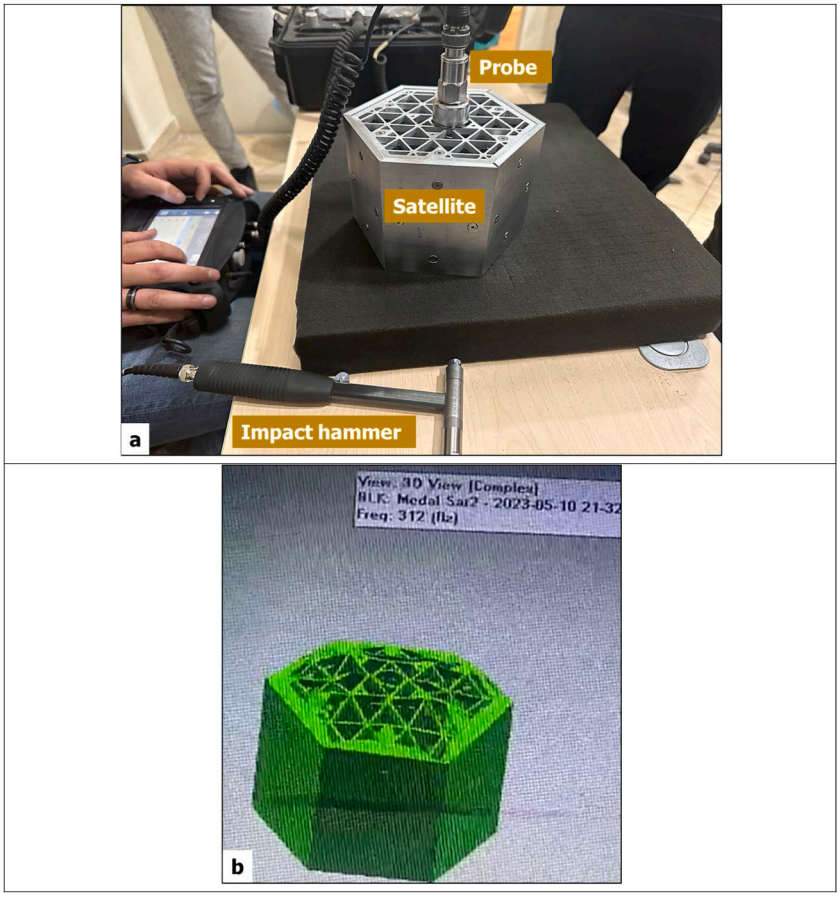

Fig. 20. Experimental vibration test setup for the manufactured satellite structure (a) and first mode shape result (b).

Declaration of competing interest

No potential conflict of interest was reported by the authors.

Acknowledgments

The authors extend their appreciation to King Saud University for funding this work through Researchers Supporting Project number (RSPD2024R711), King Saud University, Riyadh, Saudi Arabia.

Appendix A. Supplementary data

Supplementary data to this article can be found online at https://doi.org/10.1016/j.heliyon.2024.e24159.

References

[1] Reham Reda, Yasmeen Ahmed, Magdy Islam, Hossam Nabil, Mennatullah Khamis, Refaey Ahmed, Eldabaa Nada, Manar Abo Elmagd, Mohamed Abo Lila, Hady Ergawy, Alhussein Elgarf, Gerges Abed, Basic principles and mechanical considerations of satellites: a short review, Trans. Aerospace Res. 272 (3) (2023) 40–54.
[2] Craig L. Stevens, Design, Analysis, Fabrication, and Testing of a Nanosatellite Structure, Master's Thesis, Virginia Polytechnic Institute, Virginia Tech, 2002.
[3] James R. Wertz, Wiley J. Larson, Space Mission Analysis and Design, Microcosm Press and Kluwer Academic, Torrance, CA, 1992.
[4] Pat L. Mangonon, The Principles of Materials Selection for Engineering Design, Prentice Hall, Upper Saddle River, NJ, 1999.
[5] V.C.A.D. Murthy, Soundarapandian Santhanakrishnanan, Isogrid lattice structure for armouring applications, Procedia Manuf. 48 (2020) e1–e11.
[6] Thomas P. Sarafin, Wiley J. Larson, Spacecraft Structures and Mechanisms– from Concept to Launch, Microcosm Press and Kluwer Academic Publishers, Torrance, CA, 1995.
[7] E. Nathan Harris, Daniel R. Morgenthaler, Design and testing of multifunctional structure concept for spacecraft, in: The 41st Structures, Structural Dynamics, and Materials Conference and Exhibit, AIAA/ASME/ASCE/AHS/ASC, Atlanta, GA, 2000.

[8] Daniele Ciccarelli, Archimede Forcellese, Luciano Greco, Tommaso Mancia, Massimiliano Pieralisi, Michela Simoncini, Alessio Vita, Buckling behavior of 3D printed composite isogrid structures, Procedia. CIRP 99 (2021) 375–380.
[9] R.R. Meyer, O.P. Harwood, M.B. Harmon, J.I. Orlando, Isogrid Design Handbook, 1973.
[10] Ming Li, Fangfang Sun, Changliang Lai, Hualin Fan, Bin Ji, Xi Zhang, Debo Liu, Daining Fang, Fabrication and testing of composite hierarchical Isogrid stiffened cylinder, Compos. Sci. Technol. 157 (2018) 152–159.
[11] Q. Zheng, D. Jiang, C. Huang, X. Shang, S. Ju, Analysis of failure loads and optimal design of composite lattice cylinder under axial compression, Compos. Struct. 131 (2015) 885–894.
[12] Othman b Sarmad Daood Salman Dawood, Inayatullah, Razali b. Samin, Computational study of the effect of using open isogrids on the natural frequencies of a small satellite structure, Acta Astronaut. 106 (2015) 120–138.
[13] Archimede Forcellese, Valerio di Pompeo, Michela Simoncini, Alessio Vita, Manufacturing of isogrid composite structures by 3D printing, Procedia Manuf. 47 (2020) 1096–1100.
[14] Archimede Forcellese, Marco Marconi, Michela Simoncini, Alessio Vita, Environmental and buckling performance analysis of 3D printed composite isogrid structures, Procedia CIRP 98 (2021) 458–463.
[15] Sivák Peter, Ingrid Delyová, Patrícia Diabelková, Analysis of sandwich structures by the fem, Am. J. Mech. Eng. 5 (6) (2017) 243–246, https://doi.org/10.12691/ajme-5-6-2.
[16] Sadiq Emad Sadiq, Muhsin J. Jweeg, Sadeq H. Bakhy, The Effects of honeycomb parameters on transient response of an aircraft sandwich panel structure, IOP Conf. Ser. Mater. Sci. Eng. 928 (2020) 022126.
[17] Nurdina Abd Kadir, Yulfian Aminanda, Mohd Sultan, Ibrahim Shaik Dawood, Hanan Mohktar, Numerical analysis of kraft paper honeycomb subjected to uniform compression loading, IOP Conf. Series: J. Phys. Conf. 914 (2017) 012004.
[18] Z.G. Li, J.M. Wang, M. Li, F.Y. Chen, Theoretical analysis and numerical simulation of square honeycombs, J. Phys. Conf. 1777 (2021) 012042.
[19] Tiju Thomas, Gaurav Tiwari, Crushing behavior of honeycomb structure: a review, Int. J. Crashworthiness 24 (No. 5) (2019) 555–579.
[20] M.T. Mansour, K. Tsongas, D. Tzetzis, A. Antoniadis the in-plane compression performance of hierarchical honeycomb additive manufactured structures, IOP Conf. Ser. Mater. Sci. Eng. 564 (2019) 012015, https://doi.org/10.1088/1757-899X/564/1/012015.
[21] Mohammadreza Ahmadpar, Siamak Hoseinzadeh, Fardis Nakhaei, Saim Memon, Experimental modal analysis of distinguishing microstructural variations in carbon steel SA516 by applied heat treatments, natural frequencies, and damping coefficients, JMEPEG- ASM Int. 30 (2021) 9256–9261.
[22] Srikanth Raviprasad, Nagaraj Nayak, Dynamic analysis and verification of structurally optimized nano-satellite systems, J. Aero. Sci. Technol. 1 (2015) 78–90.